Mitigating *ab*-plane Critical Current Density Inhomogeneity in Bulk HTS Rings for the Generation of NMR-Grade Magnetic Fields

Michael Beck and Mark D. Ainslie, *Senior Member, IEEE*

***Abstract*—(RE)-Ba-Cu-O ring bulks, used as trapped field magnets, show great promise as a compact and lightweight source for generating the magnetic fields required for nuclear magnetic resonance (NMR). The inhomogeneities introduced by the growth process of such bulks pose a challenge to the required field uniformity for NMR. In this study, we model a stack of ring bulks with varying *ab*-plane inhomogeneity and orientation to investigate the impact on the trapped field profile following field cooled magnetization. For a pair of rings, by offsetting the growth sector boundaries (GSBs), the inhomogeneity of the circumferential field at the midplane can be reduced by up to 65% compared with aligned GSBs, for less than 0.4 % reduction in the central trapped field strength. Using two pairs of rings allows for the generation of a larger homogeneous region at the center of the bore, with a lower peak-peak variation across the measuring volume. The relative harmonic weighting of the field moves to higher orders, requiring more complex shimming coils to correct the residual field.**

***Index Terms*— Nuclear magnetic resonance, Bulk superconducting rings, high-temperature superconductors, growth sector boundary, numerical modelling, HTS modelling, field homogeneity**

I. Introduction

NUCLEAR magnetic resonance (NMR) is a key non-destructive tool for providing information on the structure, composition, and dynamic properties of a range of materials. Conventional systems, based on NbTi and Nb_3Sn solenoidal coils, are large and expensive – limiting them to specialist laboratories [1]. 'Benchtop' devices, typically based on permanent magnet (PM) sources, allow for NMR to be deployed in wider variety of locations, and to be used in applications such as the development of battery electrolyte chemistry, food safety analysis and textile quality control [2]–[4]. The use of traditional PMs as a source limits the achievable resolution due to the low field strength, and large drift due to magnet temperature fluctuations [5].

Manuscript receipt and acceptance dates will be inserted here. This work was supported by the W. D. Armstrong fund for the Application of Engineering in Medicine (corresponding author, Michael Beck) and the EPSRC Early Career Grant (corresponding author Mark D. Ainslie).

The authors are with the Bulk Superconductivity Group, Department of Engineering, University of Cambridge, Cambridge, CB2 1PZ, U.K. (email: mrb70@cam.ac.uk and mark.ainslie@eng.cam.ac.uk).

Color versions of one or more of the figures in this paper are available online at http://ieeexplore.ieee.org.

Digital Object Identifier will be inserted here upon acceptance.

Magnetized bulk high-temperature superconductors (HTS) are proven candidates for the generation of strong NMR grade magnetic fields [6]–[8] in the bore of a stack of co-axially arranged rings. Stacked pairs of ring-shaped bulks can trap fields of up to 9.78 T [9] and are readily cooled with low cost cryocoolers.

In practical bulk materials, the axisymmetry of the generated field is degraded by non-uniformities in the superconducting properties of the sample: both due to a four-fold symmetry induced from the melt-growth process [10], [11] and other cracks or defects of a random nature. This spatial dependence of material properties affects the ability of the material to trap the magnetic field [12]–[14], which for a ring-stack may introduce unwanted spherical harmonics into the magnetic field trapped within the bore.

In this study, we investigate numerically how the impact of a non-uniform superconducting current within stacked annuli may be mitigated against to improve the strength, uniformity, and stability of the trapped magnetic field following field-cooled magnetization (FCM).

II. Numerical Simulation

To analyze the electromagnetic behavior of a stack of inhomogeneous rings following FCM, a three-dimensional (3D) numerical model was constructed. As shown in Fig. 1, stacks comprised two or four rings, arranged co-axially with a 2 mm axial separation such that a cylindrical bore of constant radius and height was formed. The dimensions of the rings used were 40 mm outer diameter (OD), 16 mm inner diameter (ID), 16 mm height (H) for cases (i) and (ii); and 40/28.5/16 mm and 27.5/16/16 mm for the rings in cases (iii) and (iv). The coplanar pairs of rings in (iii) and (iv) are separated by a 1 mm thick slitted copper insert.

The electromagnetic behavior of the rings is modelled according to the 3D $\boldsymbol{H}$-formulation [15]–[17] using the magnetic field formulation (MFH) interface in the AC/DC module of COMSOL Multiphysics® 5.6. To reduce the model run-time, the stack was modelled using ¼ symmetry in the *ab*-plane.

The non-linear resistivity of the bulks is modelled according to the *E-J* power law [18], with exponent $n = 20$. The magnetic field-dependence of the critical current density, $J_c(B)$, is based on the Kim model [19], and follows

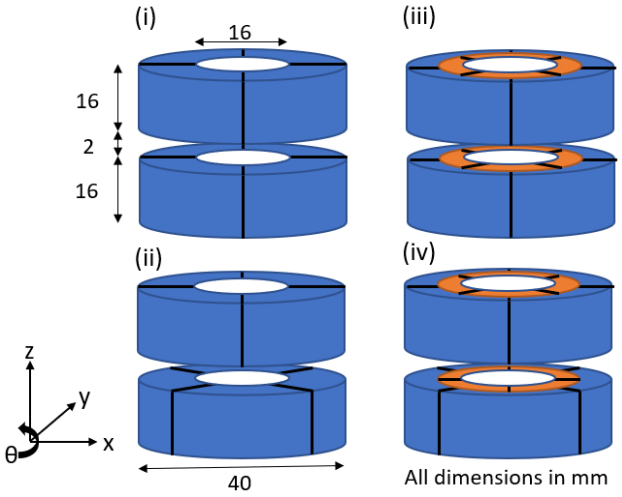

Fig. 1. The arrangements of the ring-bulk stacks for magnetization under FCM. The rings have dimensions 40/16/16 mm OD/ID/H for configurations (i) and (ii). For configurations (iii) and (iv), the inner and outer rings have dimensions 27.5/16/16 and 40/28.5/16 mm OD/ID/H respectively. The black lines denote the relative positions of the GSBs for each ring. Copper inserts not shown for clarity.

$$J_c(B) = \alpha \frac{B_0}{B + B_0} \tag{1}$$

where B_0 = 1.3 T and α = 2.16×10^8 A·m^{-2} at 65 K as in [20]. $J_c(B)$ is then varied spatially according to (2) where θ is the angle from the x-axis, and ϕ = 0 or 45° depending on the configuration.

$$J_c(B,\theta) = J_c(B)\left[\left(100 - \frac{\beta}{2}\right) + \frac{\beta}{2}\sin(4\theta + \phi)\right] \tag{2}$$

The ab-plane critical current density inhomogeneity factor, β, is set at values of 0, 30, 50, 80 or 100, such that the minimum J_c is β% lower than the maximum J_c, which remains constant between models. J_c is assumed to be independent of axial position for this investigation, although for practical samples some axial position dependence should be expected [21]. For practical rings bulks, it has been observed that J_c is greatest at the growth sector boundaries (GSBs), with a minimum value in the growth sector regions (GSRs) between these [15], [22], [23].

Four specific stack configurations are investigated here, namely:

i) Two individual rings with the GSBs aligned

ii) Two individual rings with the GSBs misaligned by 45°

iii) Two sets of two co-planar rings with the GSBs aligned in the z-direction and misaligned by 45° between rings in the same plane.

iv) Two sets of two co-planar rings with the GSBs misaligned by 45° between both the rings in the same plane, and the ring directly above/below the ring in the z-axis.

The stacks are magnetized by FCM from an initial field of 2 T at a ramp rate of 0.02 T·s^{-1} assuming isothermal conditions. The field profile is then measured at a time of t = +120 s after field removal.

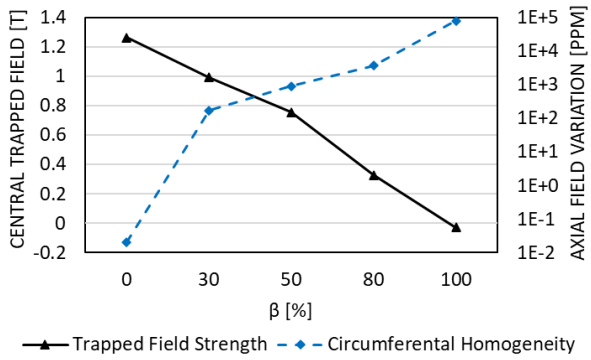

Fig. 2. The influence of J_c non-uniformity, β, on the central trapped field and circumferential field variation for configuration (i).

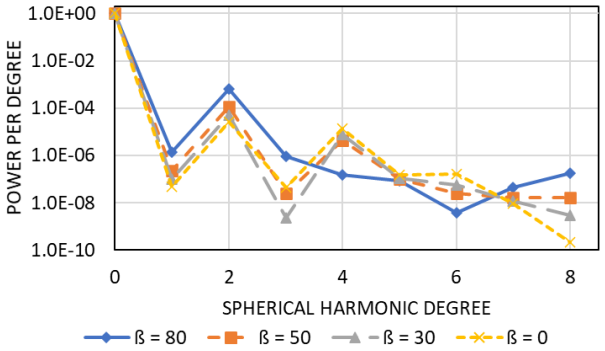

Fig. 3. The influence of J_c non-uniformity, β, on the normalized harmonic content of the sphere with radius = 4 mm at the center of configuration (i). Produced using PySHTools.

The diameter of spherical volume (DSV) within an NMR system is the region in which the field conforms to the prescribed homogeneity requirements. Real fields are non-uniform, and as such require 'shimming'. The shimming requirements – weight, degree, l, and order, m – are assessed through measurement of the spherical harmonic content of the field.

Here, the spherical harmonic data are calculated for the surface of a sphere with radius of 4 mm at the center of the ring-stack, assumed to be the target DSV. A magnetic flux density map is exported, as a '.csv' file, from COMSOL® for the DSV surface. This map is imported into Python and re-interpolated onto a uniformly mapped grid. The PySHTools package [24] is used to fit spherical harmonics, up to the 8th degree, to the output magnetic flux density of the DSV surface. For comparison, the powers are normalized to the central trapped magnetic flux density. The circular harmonic data are taken from the intersection of the DSV surface and plane z = 0 mm.

III. Results and Discussion

A. *Influence of β on Trapped Field Properties*

Firstly, we explore the influence of β on the trapped field properties for a pair of rings stacked with their GSBs aligned, as in configuration (i). As the value of β increases, the amount

of current circulating around the entirety of the bulk reduces, causing a reduction in the central trapped magnetic flux density. Fig. 2 shows that this reduction is not linear with the J_c non-uniformity, with a greater rate of reduction for $\beta > 50$. When $\beta = 100$, i.e. the critical current density = 0 A·m^{-2} in the GSRs, the circulating current is broken and a negative magnetic field is induced at the center of the ring [25].

The J_c inhomogeneity, β, has a highly non-linear influence on the field uniformity observed within the bore of the stack. The uniformity decreases rapidly for $\beta > 50$, which is observed in the variation of the field for a curve with radius 4 mm on the mid-plane, as in Fig. 2, normalized spherical harmonic powers, Fig. 3, and axial profile measurements – provided in the additional data. Therefore, ring-shaped bulk HTS for NMR must have minimal variation in the J_c values between the GSBs and GSRs. To achieve a readily shimmed mid-plane variation of 100 ppm, it is required that $\beta < 15$. Furthermore, larger rings – if produced via joining of smaller HTS bulks, e.g., using the technique proposed in [26] – will require matching of the J_c capabilities, as opposed to minimization of the joint resistance, analogous to impedance matching in radio-frequency electronics.

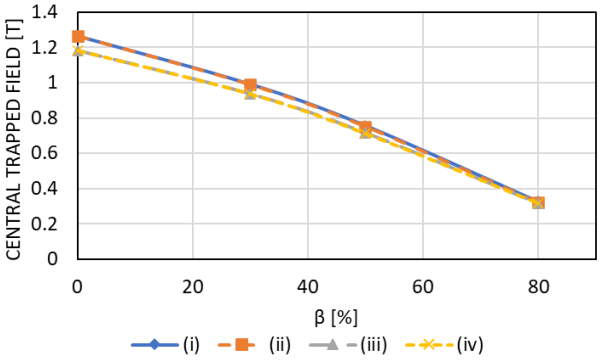

Fig. 4. The influence of J_c non-uniformity, β, and ring arrangement on the central trapped field.

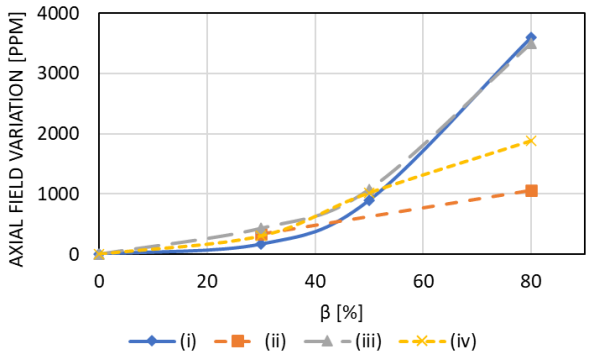

Fig. 5. The influence of J_c non-uniformity, β, on the peak-peak difference in axial field around a curve of radius 4 mm across the mid-plane of the stack.

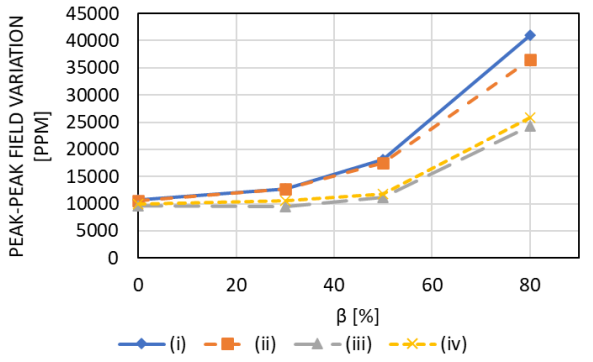

Fig. 6. The influence of J_c non-uniformity, β, and ring arrangement on peak-peak difference in axial field on a spherical surface of radius 4 mm at the center of the stack.

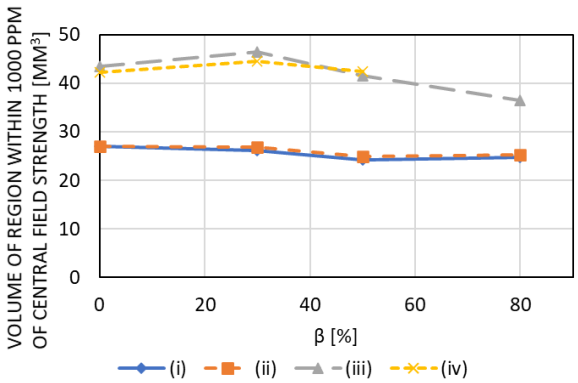

Fig. 7. The influence of J_c non-uniformity, β, and ring arrangement on the volume of the bore within 1000 ppm of the central field strength

B. *Mitigation of Field Non-Uniformity in a Multi-Bulk Stack*

Fig. 4 shows the central trapped field for configurations (i)-(iv), in which the relative orientation of the GSBs has negligible impact on the central trapped field strength. Configurations (iii) and (iv) trap a lower field compared to (i) and (ii) at low β, likely due to the reduced superconducting volume. As β increases, the difference between cases (i, ii) and (iii, iv) reduces, suggesting that the offset in co-planar rings leads to reinforcement of the field where the current is locally reduced.

The stack arrangement strongly influences other aspects of the field trapped within the bore of the stack. Arranging the rings such that the GSBs are offset 45°, as shown in Fig. 1, between the upper and lower rings, configurations (ii, iv) within the stack result in a reduction in peak-peak axial field variation, shown in Fig. 5, at the intersection of the DSV surface and z = 0 mm plane. The improvement in this field non-uniformity is more pronounced at large β, with a 75% reduction in the non-uniformity for β = 80 between cases (i), (iii) and (iv).

This improvement in field homogeneity on the mid-plane is not seen across the DSV surface. Arranging the pair of rings such that the GSBs are mis-aligned results in an improvement of up to 10% for the peak-peak field variation on the DSV surface. Constructing the stack from two pairs of rings, as in configurations (iii) and (iv), the peak-peak field variation is reduced by up to 40%. By utilizing configurations (iii) and (iv), the volume of the region within 1000 ppm of the central trapped field within the bore increased by between 47 and 78%, as shown in Fig. 7. The volume of the region within 1000 ppm of the central field appears close to independent of (i) and (ii), whereas the volume of the uniform region is

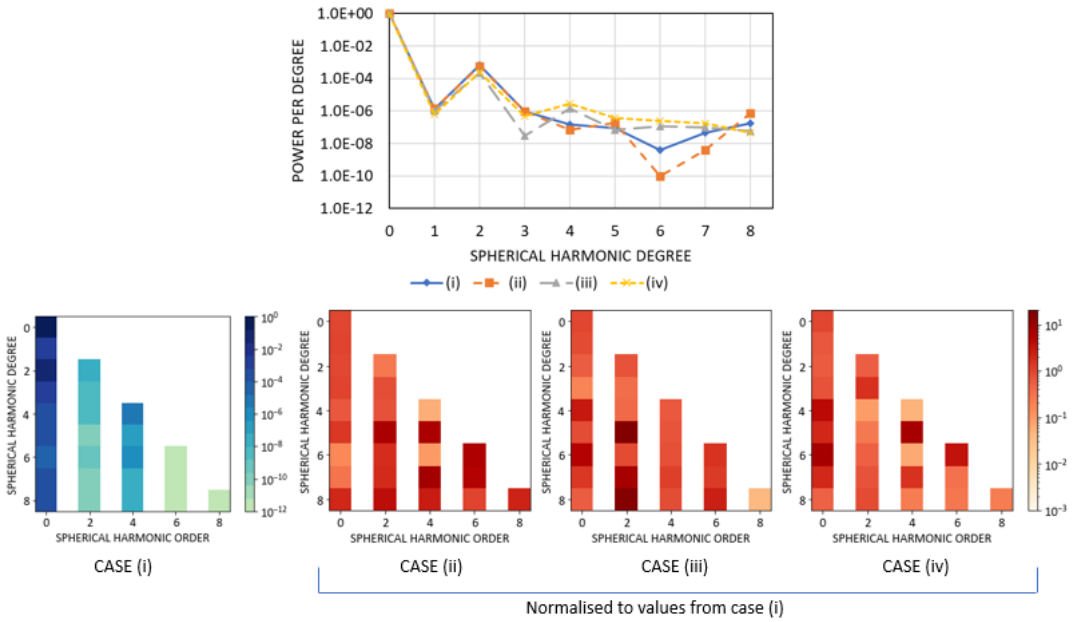

Fig. 8. The influence of stack configuration on the normalized harmonic content of the field for a sphere with radius 4 mm at the center of the stack. (a) total harmonic power per degree per harmonic degree, (b) absolute harmonic power associated with order, *m*, and degree, *l*, for configuration (i), (c-e) relative harmonic power, normalized to case (i) for cases (ii – iv) respectively, for $\beta = 80$.

strongly dependent on β for configurations (iii) and (iv). This suggests that the DSV size is limited by end effects for cases (i) and (ii), and would be mitigated by using a longer stack. In all cases, the volume of this uniform region is too small for practical use in NMR.

Fig. 8 shows how the harmonic content of the DSV varies with the ring configuration. In Fig. 8(a), the total power per degree is highest for configurations (i) and (ii) for degrees, l, < 4, suggesting suppression of the lower harmonics using the co-planar rings in configurations (iii) and (iv). Comparing this with the data in Figs. 8(d) and (e), the power of the harmonics for $l < 4$ is reduced for all orders. At the 4th degree, the power of the fundamental order increased relative to case (i), but the higher order components remain comparatively lower. This reduces the required shimming coil complexity to correct the field profile to a level suitable for NMR to the 4th order. Above the 5th order, the spherical harmonic powers within the field are elevated for configurations (iii) and (iv) when compared with (i) and (ii). Whilst the overall power per degree is comparable between cases (iii) and (iv) for $l > 4$, the relative powers of the harmonic orders are different, with a stronger 2nd spherical harmonic observed in case (iii), and stronger 4th harmonic observed for case (iv), with implications for the complexity of the shimming coil design.

Comparing the data in Figs. 7 and 8, there appears to be little correlation between the complexity of the spherical harmonic content of the bore and the size of the region in which the field is within 0.1 % of the central trapped field. Practically this would dictate arranging the rings within the stack to minimize the harmonic field content, such as to reduce the cost and complexity of the corrective shimming coils.

IV. Conclusion

For stacks of bulk HTS rings, which exhibit a spatial dependence of critical current density around the *ab*-plane due to the melt-growth process, the relative orientation of the constituent rings has a large impact on the harmonic content of the trapped field within the bore. Constructing the stack from two pairs of co-planar rings – such that the growth sector boundaries are misaligned by 45° within each pair, as seen in configurations (iii) and (iv) – results in a more homogeneous field within the bore. For these configurations, the measured inhomogeneity is reduced by up to 75 % across the midplane, and the uniform volume is increased by up to 78 %. However, the more complex manufacturing process may make these configurations infeasible.

If the use of co-planar rings is not possible, arranging the rings such that the GSBs are misaligned reduces the peak-peak variation of the field trapped within the bore by up to 65 % at the midplane, at the expense of requiring higher-order shimming coils to remove the residual field inhomogeneity. However, both solutions provide improvement in the trapped field uniformity, pre-shimming, when compared with stacked rings where all GSBs are aligned in the case where J_c is inhomogeneous around the *ab*-plane.

Data Statement

Data related to this publication are available at the University of Cambridge data repository: https://doi.org/10.17863/CAM.77587.

REFERENCES

[1] I. Armstrong-Smith, "A Briefcase Full of What?," *Education + Training*, 1985. https://theanalyticalscientist.com/techniques-tools/a-briefcase-full-of-nmr (accessed Dec. 17, 2019).

[2] J. Z. Hu *et al.*, "In situ and ex situ NMR for battery research," *J. Phys. Condens. Matter*, vol. 30, no. 46, p. 463001, Oct. 2018, doi: 10.1088/1361-648X/aae5b8.

[3] "NMR Spectroscopy in Food Safety Maintenance." https://www.news-medical.net/whitepaper/20160916/NMR-Spectroscopy-in-Food-Safety-Maintenance.aspx (accessed Sep. 28, 2021).

[4] S. Haslinger *et al.*, "Solid-state NMR method for the quantification of cellulose and polyester in textile blends," *Carbohydr. Polym.*, vol. 207, pp. 11–16, Mar. 2019, doi: 10.1016/j.carbpol.2018.11.052.

[5] E. Danieli *et al.*, "Small magnets for portable NMR spectrometers," *Angew. Chemie - Int. Ed.*, vol. 49, no. 24, pp. 4133–4135, Jun. 2010, doi: 10.1002/anie.201000221.

[6] T. Nakamura *et al.*, "Development of a superconducting magnet for nuclear magnetic resonance using bulk high-temperature superconducting materials," *Concepts Magn. Reson. Part B Magn. Reson. Eng.*, vol. 31, no. 2, pp. 65–70, Apr. 2007, doi: 10.1002/cmr.b.20083.

[7] K. Ogawa *et al.*, "Development of a magnetic resonance microscope using a high T_c bulk superconducting magnet," *Appl. Phys. Lett.*, vol. 98, no. 23, 2011, Art. no. 234101, doi: 10.1063/1.3598440.

[8] T. Nakamura *et al.*, "Development of a superconducting bulk magnet for NMR and MRI," *J. Magn. Reson.*, vol. 259, pp. 68–75, 2015, doi: 10.1016/j.jmr.2015.07.012.

[9] O. Vakaliuk *et al.*, "Trapped field potential of commercial Y-Ba-Cu-O bulk superconductors designed for applications," *Supercond. Sci. Technol.*, vol. 33, no. 9, p. 9, 2020, Art. no. 095005 doi: 10.1088/1361-6668/ab9fc4.

[10] M. Sekino *et al.*, "Concentric slitting of a ring-shaped bulk superconductor for a reduction in circumferential inhomogeneity of the trapped magnetic field," *IEEE Trans. Appl. Supercond.*, vol. 21, no. 3, pp. 1588–1591, Jun. 2011, doi: 10.1109/TASC.2010.2091614.

[11] S. Nariki, H. Teshima, and M. Morita, "Development of High-Performance QMG Bulk Magnets for High Magnetic Field Engineering Applications," *IEEE Trans. Appl. Supercond.*, vol. 26, no. 3, Apr. 2016, Art no. 7200404, doi: 10.1109/TASC.2016.2537382.

[12] Y. Komi, M. Sekino, and H. Ohsaki, "Three-dimensional numerical analysis of magnetic and thermal fields during pulsed field magnetization of bulk superconductors with inhomogeneous superconducting properties," *Phys. C Supercond. its Appl.*, vol. 469, no. 15–20, pp. 1262–1265, Oct. 2009, doi: 10.1016/j.physc.2009.05.121.

[13] H. Fukai *et al.*, "The effect of inhomogeneous flux penetration into bulk superconductor by pulsed field magnetization," *Supercond. Sci. Technol.*, vol. 18, no. 9, pp. 1179–1182, Sep. 2005, doi: 10.1088/0953-2048/18/9/006.

[14] H. H. Song *et al.*, "Evaluation of inhomogeneities of bulk YBCO superconductors using pulsed field magnetization," *Phys. C Supercond. its Appl.*, vol. 420, no. 1–2, pp. 51–55, Mar. 2005, doi: 10.1016/j.physc.2005.01.007.

[15] M. D. Ainslie *et al.*, "Modelling and comparison of trapped fields in (RE)BCO bulk superconductors for activation using pulsed field magnetization," *Supercond. Sci. Technol.*, vol. 27, no. 6, 2014, Art no. 065008 doi: 10.1088/0953-2048/27/6/065008.

[16] M. D. Ainslie *et al.*, "Numerical modelling of mechanical stresses in bulk superconductor magnets with and without mechanical reinforcement," *Supercond. Sci. Technol.*, vol. 32, no. 3, Feb. 2019, Art no. 034002, doi: 10.1088/1361-6668/aaf851.

[17] K. Zhang *et al.*, "Fast and efficient critical state modelling of field-cooled bulk high-temperature superconductors using a backward computation method," *Supercond. Sci. Technol.*, vol. 33, no. 11, Nov. 2020, Art no. 114007, doi: 10.1088/1361-6668/ABB78A.

[18] C. J. G. Plummer and J. E. Evetts, "Dependence of the shape of the resistive transition on composite inhomogeneity in multifilamentary wires," *IEEE Trans. Magn.*, vol. 23, no. 2, pp. 1179–1182, 1987, doi: 10.1109/TMAG.1987.1064997.

[19] P. W. Anderson and Y. B. Kim, "Hard superconductivity: Theory of the motion of abrikosov flux lines," *Rev. Mod. Phys.*, vol. 36, no. 1, pp. 39–43, 1964, doi: 10.1103/RevModPhys.36.39.

[20] S. Zou, V. M. R. Zermeno, and F. Grilli, "Influence of parameters on the simulation of HTS bulks magnetized by pulsed field magnetization," *IEEE Trans. Appl. Supercond.*, vol. 26, no. 4, Jun. 2016, Art no. 4702405, doi: 10.1109/TASC.2016.2535379.

[21] J. Zheng *et al.*, "Modeling study on high-temperature superconducting bulk's growth anisotropy effect on magnetization and levitation properties in applied magnetic fields," *Supercond. Sci. Technol.*, vol. 34, no. 3, p. 11, Mar. 2021, Art no. 035011, doi: 10.1088/1361-6668/abdba5.

[22] C. D. Dewhurst, W. Lo, and D. A. Cardwell, "Distribution of critical current density in large $YBa_2Cu_3O_{7-\delta}$ grains fabricated using seeded peritectic solidification," *IEEE Trans. Appl. Supercond.*, vol. 7, no. 2, pp. 1925–1928, 1997, doi: 10.1109/77.620962.

[23] M. D. Ainslie *et al.*, "Pulsed field magnetization of 0°-0° and 45°-45° bridge-seeded Y-Ba-Cu-O bulk superconductors," *Supercond. Sci. Technol.*, vol. 28, no. 12, Oct. 2015, Art no. 125002, doi: 10.1088/0953-2048/28/12/125002.

[24] M. A. Wieczorek and M. Meschede, "SHTools: Tools for Working with Spherical Harmonics," *Geochemistry, Geophys. Geosystems*, vol. 19, no. 8, pp. 2574–2592, 2018, doi: 10.1029/2018GC007529.

[25] H. Mochizuki *et al.*, "Trapped Field Characteristics and Fracture Behavior of REBaCuO Bulk Ring during Pulsed Field Magnetization," *IEEE Trans. Appl. Supercond.*, vol. 26, no. 4, Jun. 2016, Art no. 6800205, doi: 10.1109/TASC.2015.2513415.

[26] J. V. J. Congreve *et al.*, "A reliable technique to fabricate superconducting joints between single grain, Y–Ba–Cu–O bulk superconductors," *Supercond. Sci. Technol.*, vol. 34, no. 9, p. 094003, Aug. 2021, Art no. 094003, doi: 10.1088/1361-6668/ac19f1.